

GNSS NLOS and Multipath Error Mitigation using Advanced Multi-Constellation Consistency Checking with Height Aiding

Ziyi Jiang, Paul D Groves
University College London, United Kingdom

BIOGRAPHY

All authors are members of the Space Geodesy and Navigation Laboratory (SGNL) at University College London (UCL).

Dr Ziyi Jiang is a research fellow at UCL, currently specialising in multipath and NLOS mitigation research. He completed his PhD at UCL on digital-route-model-aided integrated satellite navigation and low-cost inertial sensors for high-performance positioning on the railways. He also holds a BEng in measuring and control technology from Harbin Engineering University, China (ziyi.jiang@ucl.ac.uk).

Dr Paul Groves is a Lecturer (academic faculty member) at UCL, where he leads a program of research into robust positioning and navigation. He joined in 2009, after 12 years of navigation systems research at DERA and QinetiQ. He is interested in all aspects of navigation and positioning, including multi-sensor integrated navigation, improving GNSS performance under challenging reception conditions, and novel positioning techniques. He is an author of about 50 technical publications, including the book *Principles of GNSS, Inertial and Multi-Sensor Integrated Navigation Systems*. He is a Fellow of the Royal Institute of Navigation and an associate editor of both *Navigation: Journal of the ION* and *IEEE Transactions on Aerospace and Electronic Systems*. He holds a BA/MA and a DPhil in physics from the University of Oxford (p.groves@ucl.ac.uk).

ABSTRACT

High sensitivity multi-constellation GNSS receivers can dramatically improve the satellite availability in an urban environment. However, positioning accuracy remains a challenge because of blockage, reflection and diffraction of signals by buildings. In typical urban positioning scenarios, the receiver often receives a mixture of non-line-of-sight (NLOS) signals, multipath-contaminated direct line-of-sight (LOS) signals, and clean direct-LOS signals. Multi-constellation GNSS allows maximising the positioning accuracy by selecting only those signals that are least contaminated by multipath and NLOS propagation to form the navigation solution. A technique

exploring the consistency among received signals using randomly draw subsets of all available signals is proposed in this research. The implementation of the algorithm follows an estimation scheme known as RANdom SAmple Consensus (RANSAC). A pre-defined cost function is firstly used to select the best available subset of measurements. A reference solution is produced from the best available subset. The “residuals” of all received signals, i.e. the differences between the observed measurements and the predictions from the reference solution, are examined. The examination features a receiver autonomous integrity monitoring (RAIM) like statistical test based on specific distributions. A final solution is produced from measurements passed the examination plus the best available subset. In addition, height aiding from a terrain elevation database is used as an additional ranging measurement to further enhance the positioning performance. Two GPS/GLONASS data sets collected from different urban areas of central London were used for testing. Different versions of the cost function and the effect of introducing height aiding are tested. The results show an improvement of positioning accuracy over conventional least-squares algorithm and previous consistency-checking algorithm through reduction of the impact of multipath and NLOS propagation errors.

1. INTRODUCTION

The urban environment presents two major challenges to GNSS signal reception. Firstly, buildings and other obstacles, such as buses, block the direct line-of-sight to many satellites, reducing the number in view. The remaining signals often have poor geometry, degrading the positioning accuracy [1]. The second problem is that urban environments contain many flat and reflective surfaces that reflect GNSS signals. Reception of these reflected signals results in significant positioning errors.

Where the direct signal is blocked and the signal is received only via reflections, this is known as non-line-of-sight (NLOS) reception. Where the signal is received through multiple paths, this is known as multipath interference. NLOS reception and multipath interference are often grouped together as “multipath”. However, they are actually separate phenomena that produce very

different ranging errors. NLOS reception and multipath interference can occur separately, but also occur together whenever a signal is received via multiple reflected paths but not directly.

NLOS reception results in a pseudo-range measurement error equal to the additional path delay, the difference between length of the path taken by the reflected signal and the (blocked) direct path between satellite and receiver. This error is always positive and, although typically tens of metres, is potentially unlimited. Signals received via distant tall buildings can exhibit errors of more than a kilometre. NLOS signals can be nearly as strong as the directly received signals, but can also be very weak. As high-sensitivity receivers can acquire much weaker signals, their use can significantly increase the number of NLOS signals received.

Where multipath interference to directly received signals occurs, the reflected signals distort the code correlation peak within the receiver such that the code phase of the direct line-of-sight (LOS) signal cannot be accurately determined by equalising the power in the early and late correlation channels. The resulting code tracking error depends on the receiver design as well as the direct and reflected signal strengths, path delay and phase difference, and can be up to half a code chip [2, 3, 4]. Carrier-phase tracking errors are limited to a quarter of a wavelength (assuming the direct LOS signal is stronger than the reflections).

Although the NLOS reception and multipath interference affect both code- and carrier-phase observations, code-phase contamination is on a much larger scale and is usually the dominant error source for urban positioning situations.

Several methods exist for mitigating multipath interference and NLOS reception. However, they all have their limitations. Techniques may be classified as antenna-based, receiver-based and post-receiver, and may be used in combination. Antenna-based techniques such as beam-forming antenna arrays [5], ground planes and choke rings are usually bulky and expensive. The application of dual-polarisation antenna [6] can be used to detect the NLOS reception. Receiver-based techniques, summarised in [2], that sharpen the peak of the code correlation function are relatively expensive to implement and have no effect on NLOS signal reception.

Post-receiver techniques operate using the pseudo-range, carrier-phase and carrier-power-to-noise density ratio, C/N_0 , measurements prior to the positioning calculation. Multipath interference may be detected and mitigated by comparing measurements on different frequencies from the same satellite [6]. However, these techniques are of little use for mitigating NLOS reception.

The assumption held by lots of conventional techniques is that only a single GNSS constellation is used. However,

multi-constellation GNSS provides access to many more signals. Accuracy can thus be maximised by selecting only those signals least contaminated by multipath and NLOS propagation to form the navigation solution and discarding the rest. With single-constellation GNSS, there is limited scope to do this without compromising the availability of a position solution with adequate geometry, particularly in challenging environments, such as city centres.

NLOS reception may be detected using a dual-polarisation antenna [7], an antenna array [8], or a panoramic camera [9, 10]. However, these techniques all require additional hardware, increasing the cost, size and power consumption of the user equipment.

The focus of this paper is signal selection by consistency checking, whereby measurements from different satellites are compared with each other to identify the NLOS and multipath-contaminated signals. Consistency checking can operate using only one measurement per satellite, though sensitivity is improved by using multiple measurements. It may thus be used either as a low-cost alternative to the other methods or as an augmentation to improve overall robustness.

Furthermore, the urban mapping activities carried out by commercial companies have already expanded beyond the scope of traditional sense of a 2D map of only streets and buildings. 3D maps with height information can be easily obtained on consumer mobile devices. Indoor mapping is also under rapid development. Therefore, the effect of combining height aiding with the consistency-checking algorithm is also investigated in this research.

Section 2 reviews the basic principles of consistency checking. A summary of previous research is also included along with the rationale of the new consistency-checking algorithm. Section 3 describes the implementation of the new algorithm. Different versions of the cost functions and the formulation of height aiding are also given. Section 4 shows the test results obtained using two GPS/GLONASS data sets collected from different parts of central London. Finally, the conclusions of the research on the new algorithm and suggestions for future improvements are given in Section 5.

Consistency-based NLOS and multipath detection, and height aiding may both be implemented as part of an intelligent urban positioning system using multi-constellation GNSS with 3D mapping [11], alongside conventional GNSS positioning and shadow matching [12].

2. BACKGROUND ON CONSISTENCY CHECKING

The principle of consistency checking is that NLOS and multipath-contaminated measurements produce a less consistent navigation solution than clean direct-LOS

measurements. In other words, if position solutions are computed using combinations of signals from different satellites, those obtained using only the multipath-free signals should be in greater agreement than those that include multipath-contaminated and NLOS measurements. Thus these measurements may be identified through various consistency-checking based approaches. By eliminating these contaminated measurements, a more accurate position solution can be produced. The same principle is used for fault detection in receiver autonomous integrity monitoring (RAIM) [13, 14]. The difference is that, in RAIM, the object is to detect and exclude faulty data and to calculate protection levels, whereas here, the aim is to identify the set of measurements least affected by multipath and NLOS propagation.

Previous research on using consistency-checking to mitigate NLOS reception and multipath interference errors [15] has shown that this technique can identify and eliminate NLOS signals when most of the other received signals are direct LOS with minimal multipath interference, but is less reliable in more challenging environments. The processing scheme used for that study operates in a similar “top down” mode to RAIM, starting from the overall residuals from a least-squares solution obtained from all available measurements. The algorithm is usually implemented as an iterative process. Problematic signals are eliminated and residuals are recomputed until either the test is passed or insufficient signals remain. The elimination criteria can also be adjusted to reflect the assumption that a NLOS signal is always delayed with respect to the corresponding direct signal.

The underlying assumptions of such a “top down” implementation of consistency checking are:

- Measurement errors follow a zero-mean Gaussian distribution;
- Faulty signals are the minority amongst the received signals; and
- The errors on different signals are independent of each other.

This, however, is not always true under extreme NLOS and multipath conditions, such as typical urban canyons. When only a small part of sky can be seen and a large number of highly reflective objects are present around the receiver location, a set of received signals may be found that are consistent amongst them but still produce an erroneous position solution. Without further information on the signals or surrounding environment, the consistency-checking method struggles to work with the biased residuals.

Another assumption of the hypothesis testing is that the measurement errors follow a zero-mean Gaussian distribution; hence the core of the testing is a chi-square test examining the normality of the measurement

residuals. However, errors caused by extreme multipath and NLOS signals do not become white over time as shown in previous research [15]. Instead, a more systematic pattern is usually expected. Therefore, when only consistency checking methods are applied, the accuracy improvement can sometimes be limited.

It is also demonstrated from the previous study that when a suitable weighting scheme is combined with the consistency checking method, it is possible to improve the accuracy and reliability of the solution. This is because NLOS signals usually exhibit a lower C/N_0 value than direct-LOS signals.

Residuals produced from a weighted least-squares solution alone do not show the quality of each signal when multiple erroneous signals are present. This is because least-squares as an estimation algorithm has a particular low break point, i.e. the method performs poorly on data sets containing a high ratio of erroneous outliers [16]. In order to ensure a high-quality solution and useful residuals, the noise level on the different measurements must be at a similar level. However, the satellite ranging measurements produced in an urban environment do not meet this requirement. Some subset of measurements may be consistent within only a small group instead of the whole set. This leads to groups of subsets exhibiting different noise level to each other, and results in the residuals information to be biased.

Therefore it is necessary to understand the noise level structure within the whole measurement set before putting it through a least-squares estimator. In this way, it reveals more information on each individual measurement that could be potentially used for error correction, and ensures the usefulness of least-squares residuals for any further attempt to improve the estimation accuracy.

Because some measurements could exhibit consistency within a small subset of all available measurements, it naturally follows to make use of these subsets. A subset that consists only of the minimum number of measurements required to produce an exact solution, can be used to provide a reference for the remaining measurement to be compared against.

Figure 1 shows an example of the position errors of all possible subsets of 5 measurements at a single epoch in a dense urban location. The errors are plotted in easting and northing directions, and the truth was obtained using conventional surveying techniques.

As the dots are plotted with a certain level of transparency, it can be immediately observed from the figure that consistency among subsets of measurements results in some area having a higher density of solutions than others. It can also be seen that a minority of the solutions, shown within the red square, do show a better accuracy than most of the others. This indicates, firstly, that the majority of signals in this scenario are

contaminated; and, secondly, that it is possible to provide a better reference against which individual measurements may be compared by properly selecting a subset of the measurements.

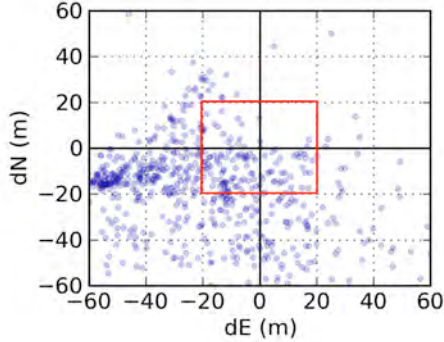


Figure 1: An example of position cluster produced from all possible subsets of available measurements

Based on this reasoning, we propose a new processing scheme for consistency-based NLOS and multipath error mitigation. The new scheme incorporates a technique known as RANdom SAMple Consensus (RANSAC), which utilises random-draw subsets of the measurements and a probability-based stopping criterion for efficiency. The RANSAC technique that was previously proposed for computer image processing to deal with data sets with high portion of outliers [16]. Details of the algorithm are presented in Section 3.

3. ADVANCED CONSISTENCY CHECKING ALGORITHMS

This section introduces the implementation of the new advanced consistency checking algorithms. Section 3.1 firstly formulates the basic least-squares problem within the GNSS context and the modeling for GPS/GLONASS code-phase pseudorange measurements. Section 3.2 briefly reviews the implementation scheme of a “Top down” recursive consistency checking algorithm. Section 3.3 describes the estimation process of the new RANSAC-based “bottom up” consistency-checking algorithm. Lastly, section 3.4 shows how the height measurement is modeled and incorporated with satellite pseudorange measurements.

3.1. FORMULATION OF ESTIMATION PROBLEM

Assuming n measurements are available, m unknowns need to be determined, and $n \geq m$, the basic GNSS measurement and solution relationship can be described by an over-determined system of linear equations in the form of

$$\tilde{\mathbf{z}} = \mathbf{G}\mathbf{x} + \mathbf{e} \quad (1)$$

where $\tilde{\mathbf{z}}$ is a $n \times 1$ measurement vector; \mathbf{x} is a $m \times 1$ state vector; \mathbf{G} is a $n \times m$ measurement matrix; And \mathbf{e} is the measurement error vector ($n \times 1$).

For the case of positioning with satellite-ranging measurements, the measurement vector $\tilde{\mathbf{z}}$ accommodates the differences between the actual measured pseudorange and the predicted ranges based on a nominal user position, and the state vector \mathbf{x} includes estimates of the user position plus the receiver clock error and/or inter-constellation timeframe differences ($n=4$ or 5). The measurement matrix \mathbf{G} contains the geometry information of the available constellation that links the measurements to the solution. The measurement error is a combination of all unaccounted-for ranging errors such as residual satellite orbit and clock, residual atmospheric effects and multipath etc.

The well-known least-squares solution of the problem presented in Equation (1) can be written as [6]

$$\hat{\mathbf{x}} = (\mathbf{G}^T \mathbf{G})^{-1} \mathbf{G}^T \tilde{\mathbf{z}} \quad (2)$$

where $\hat{\mathbf{x}}$ is the least-squares solution of the state vector. A $n \times 1$ residual vector \mathbf{v} can be calculated using a predicted measurement vector $\hat{\mathbf{z}}$, which can be calculated with

$$\hat{\mathbf{z}} = \mathbf{G}\hat{\mathbf{x}} \quad (3)$$

Hence, the residual vector \mathbf{v} is obtained using

$$\mathbf{v} = \tilde{\mathbf{z}} - \hat{\mathbf{z}} = [\mathbf{I} - \mathbf{G}(\mathbf{G}^T \mathbf{G})^{-1} \mathbf{G}^T] \tilde{\mathbf{z}} \quad (4)$$

A weight matrix $\mathbf{W} (n \times n)$ can be applied to the estimated state vector as in Equation (2):

$$\hat{\mathbf{x}} = (\mathbf{G}^T \mathbf{W} \mathbf{G})^{-1} \mathbf{G}^T \mathbf{W} \tilde{\mathbf{z}} \quad (5)$$

Here, \mathbf{W} is defined as

$$\mathbf{W} = \text{diag}(\sigma_1^2, \dots, \sigma_j^2, \dots, \sigma_n^2)^{-1} \quad (6)$$

where σ_j is the modelled error standard deviation of each measurement. The difference between two weighting schemes lies in the modelling of σ_j .

The signal carrier power to noise density ratio, C/N_0 , is an effective indication of the received signal strength, which is normally lower for reflected signals. One of the models used to form σ_j as a function of the measured C/N_0 in this research is described by [14]:

$$\sigma_j^2 = c \cdot 10^{-\frac{C/N_0}{10}} \quad (7)$$

where c is the model parameter, and is a constant depending on receiver and antenna types. Although antenna and receiver designs can affect the absolute C/N_0 value, a relative comparison of C/N_0 among the received signals can still indicate their quality.

The corrected GNSS pseudorange measurements obtained from for the satellites of the different constellations may be written as

$$\tilde{\rho}_G = r + c_{light} \cdot \delta t_u + \tilde{\epsilon}_G \quad (8)$$

$$\tilde{\rho}_R = r + c_{light} \cdot (\delta t_u + \delta t_{G-R}) + \tilde{\epsilon}_R \quad (9)$$

where $\tilde{\rho}_G$ and $\tilde{\rho}_R$ are, respectively, the corrected GPS and GLONASS pseudorange measurement after the troposphere and ionosphere corrections have been applied to the measured ranges; r is the true geometric range between the satellite at the signal emission time and the receiver at the signal reception time; c_{light} is the speed of light; δt_u is the receiver clock bias relative to GPS time at the signal reception time; δt_{G-R} in Equation (6) is the timeframe difference between GPS and GLONASS; $\tilde{\epsilon}_G$ and $\tilde{\epsilon}_R$ consists of residuals after applying corrections from the broadcast navigation data and other residual multipath and atmospheric errors.

Equations (8) and (9) are both incorporated into the linear system described by Equation (1) to solve for the receiver position.

3.2. “TOP DOWN” CONSISTENCY-CHECKING APPROACH

A brief illustration of the “Top down” recursive checking process is shown in Figure 2. The least-squares solution is firstly computed as the starting point of the checking. A test statistic is calculated using the measurement residuals. The result of the comparison between the test statistics and the threshold indicates whether an inconsistency is identified among the available measurements.

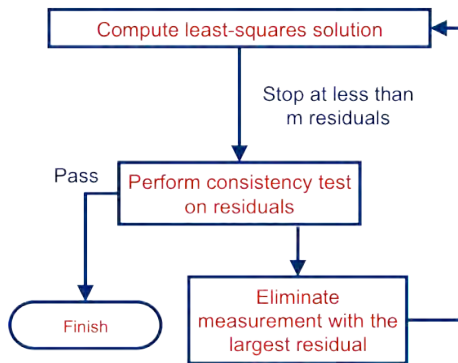


Figure 2: The “Top down” approach

A failed test result will lead to the elimination of the measurement with the largest normalised residual. A new least-squares solution is recomputed after each elimination, hence producing a new set of residuals. The test statistics and the threshold are all recomputed with the new residuals. This recursive procedure carries on

until the test is passed, or insufficient measurements remain. Further details may be found in [15].

3.3. “BOTTOM UP” CONSISTENCY-CHECKING APPROACH

The implementation scheme of the “Bottom up” approach follows the conventional RANSAC scheme, which consists of two essential steps that repeat as an iterative process as illustrated in Figure 3:

- *Hypothesize*: A Minimal Sample Set (MSS) is randomly selected from all available measurements at one epoch. The size of the MSS is the smallest sufficient to determine a reference positioning solution (4 or 5 depending on MSS constellation constitution);
- *Test*: The consistency is then determined using the “residuals” of all remaining measurements. A “residual” under this context is defined as the difference between the observed measurement and its prediction produced based on the reference solution calculated using the MSS.

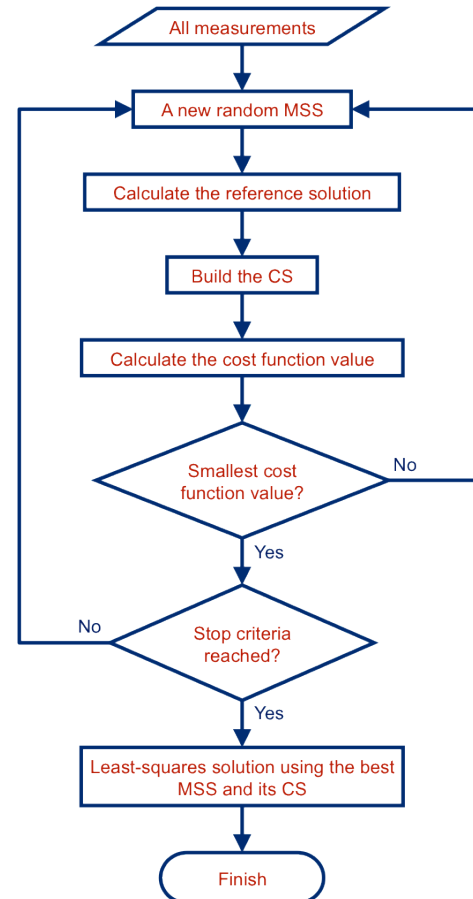


Figure 3: The “Bottom up” approach

Those measurements whose residuals fall within a certain threshold are assumed to be consistent with the reference solution and are known as inliers. The set of inliers is referred to as the Consensus Set (CS) for the MSS. A predefined cost function is used to assess the quality of

each MSS. The goal of the iteration is to achieve a minimisation of the cost function, i.e. find the best quality MSS, when it finishes. The iteration terminates when the probability of finding a better MSS drops below a certain threshold.

For the i^{th} MSS, comprising the measurements $\tilde{\mathbf{z}}^i \in \tilde{\mathbf{z}}$, its reference solution $\hat{\mathbf{x}}^i$ is generated following Equation (2):

$$\hat{\mathbf{x}}^i = ((\mathbf{G}^i)^T \mathbf{G}^i)^{-1} (\mathbf{G}^i)^T \tilde{\mathbf{z}}^i \quad (8)$$

Except that \mathbf{G}^i is the partial measurement matrix, containing only those rows of \mathbf{G} that apply to the measurements within the i^{th} MSS, and the reference solution is exact. The set of “residuals”, \mathbf{e}^i defined as $[e_1^i, e_2^i, \dots, e_n^i]^T$, is calculated using

$$\mathbf{e}^i = \tilde{\mathbf{z}}^i - \hat{\mathbf{z}}^i = \tilde{\mathbf{z}}^i - \mathbf{G}^i \hat{\mathbf{x}}^i \quad (9)$$

Assuming the “residual” of all the measurements follows a known distribution, the “residuals” can be tested for the goodness-of-fit based on a threshold δ . In this paper, a Gaussian distribution is assumed. However, the RANSAC method allows a more realistic distribution to be employed in its place.

Under the hypothesis that there are no contaminated measurements, let q be the probability of sampling a MSS for which all of the remaining measurements are inliers. The probability of picking a MSS for which there is at least one outlier is $1-q$. The probability of constructing h MSSs and all of them leading to the detection of outliers is $(1-q)^h$. The size of h should be large enough that $(1-q)^h < \alpha$ where α is the false alarm probability. The relationship can be rewritten as:

$$h \leq \left\lceil \frac{\log \alpha}{\log(1-q)} \right\rceil \quad (10)$$

where $\lceil x \rceil$ denotes the smallest integer larger than x . Therefore with a given false alarm rate α , the stop criteria is defined as:

$$T_{iter} = \left\lceil \frac{\log \alpha}{\log(1-q)} \right\rceil, \quad (11)$$

where T_{iter} is the maximum number of MSSs generated.

If each individual in all measurements n has the same probability of been selected for a size m MSS, the q can be written as

$$q = \frac{\binom{\hat{n}_{inlier}}{m}}{\binom{n}{m}} \quad (12)$$

where \hat{n}_{inlier} is an estimate of the number of inliers available within all the measurements, and $\binom{a}{b}$ is the number of b -element combinations of a set a . Following [16], the size of the current best CS can be used as a valid approximation of \hat{n}_{inlier} .

The cost function $C^i(\cdot)$ to assess the quality of the MSS and its associated CS can be defined in various forms. A common RANSAC cost function, based purely on the size of individual “residual”, is defined by [16] as

$$C^i(\tilde{\mathbf{z}}) = \sum_{j=1}^n \rho(e_j^i, \delta) \quad (13)$$

Where:

$$\rho(e_j^i, \delta) = \begin{cases} e_j^i, & e_j^i \leq \delta \\ \delta, & otherwise \end{cases} \quad (14)$$

For the case of GNSS, different weighting factors can also be applied to enhance the probability of generating an optimal MSS and CS. To apply a weighting based on the measured C/N_0 values of the individual measurements, Equation (14) becomes

$$\rho(e_j^i, \delta) = \begin{cases} \frac{e_j^i}{\sigma_j}, & e_j^i \leq \delta \\ \frac{\delta}{\sigma_j}, & otherwise \end{cases}, \quad (15)$$

where σ_j is as defined by Equation (7) for the normal least-squares solution.

Lastly, once a best MSS and its CS have been identified through the CS, they can then be used along with an appropriate weighting scheme to produce a new least-squares position solution.

3.4. HEIGHT AIDING

The height information obtained from a 3D city model is integrated into the final least-squares solution produces from the best CS. The height measurement can be modelled as an additional range measurement $\tilde{\rho}_H$ from the centre of the earth to the priori receiver position. With

reference to Equations (8) and (9), the model can therefore be written as:

$$\tilde{\rho}_H = r + \tilde{\epsilon}_H \quad (15)$$

The unit vector \hat{u}_H , used within the measurement matrix, can be obtained using

$$\hat{u}_H = \frac{\hat{r}_u}{|\hat{r}_u|} \quad (16)$$

where \hat{r}_u is the a priori receiver position vector from the center of the Earth. The least-squares position solution is then determined in the same way as for an all-satellite solution, except that the height-aiding row of the measurement matrix has a zero in the receiver clock column.

4. TEST RESULTS AND DISCUSSION

Two sets of urban data have been used to test the algorithm. Each data set contains GPS/GLONASS data collected in a different location in the City area of Central London.

The positioning errors using a conventional weighted least-squares solution only, using the “Top down” consistency checking method and using “Bottom up” approach to consistency checking, have been compared for each data set. Note that all three methods make use of C/N_0 weighting. In addition, the percentages of positioning errors exceeding a threshold are also compared for all three algorithms. Finally, results from the height-assisted weighted least-squares solution and the “Bottom up” solution are used to test the effect of height aiding.

Note that the results from [15] already indicate that the “Top down” approach works well under moderate urban conditions, but is less reliable for severe urban conditions. While the new “Bottom up” approach generally outperforms the old method, the two scenarios presented here are chosen to demonstrate severe urban conditions where the “Top down” approach fails to perform and study the behaviour of the new algorithm under the same circumstances.

4.1. TEST 1

The first test data was collected near Moorgate underground station on 8th April 2011. The duration of the data is 38 minutes. Figure 4 shows a comparison of positioning solutions produced with three algorithms in the first 10 minutes of data. A yellow pin in the picture marks out the truth point, T3. The truth was established using traditional surveying methods and is accurate at cm-level (the traversing accuracy was 1 in 56000). The red triangles in the figure are the least-squares position

solutions without consistency checking; the blue triangles show the solutions with “Top down” consistency checking; and the green triangles show the positions obtained using the “Bottom up” consistency-checking approach. The smaller circle has a 10-metre radius, and the larger circle a 20-metre radius.

The overall position error of all three algorithms throughout the whole data set is shown in Figure 5. The red lines in the figure represent the least-squares solution without consistency checking; the blue lines show the “Top down” solution; and the green line are the “Bottom up” solution. The RMS easting, northing and vertical positioning errors are also presented in Table 1.



Figure 4: The first 10 min positioning solution for test 1

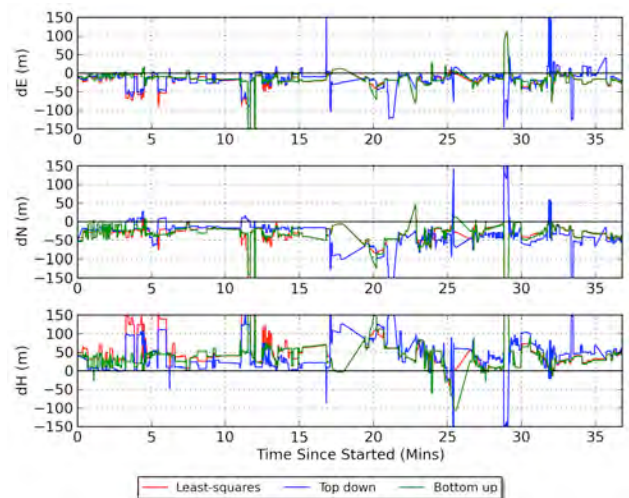


Figure 5: The positioning error comparison of the three algorithms for test 1

	dE (m)	dN (m)	dH (m)
Least-squares	29.0	43.1	70.4
“Top down”	30.4	46.0	62.2
“Bottom up”	24.1	43.2	59.5

Table 1: The RMS positioning error comparison of the three algorithms for test 1

From the RMS error figures in Table 1, while no significant improvements are observed from either the

“Top down” or “Bottom up” consistency checking approaches in the northing direction, a 17% improvement is achieved in the easting direction by using the “Bottom up” consistency-checking approach. Both algorithms produce a similar improvement to the height error.

Based on the information in Figure 4, 5 and Table 1, it is shown that “Bottom up” consistency-checking method can improve the accuracy even under difficult urban situations where the conventional and “Top down” algorithms struggle. More importantly, as can be seen by looking at the number of position solutions outside the 20m circle in Figure 5, the “Bottom up” algorithm is less prone to producing erroneous solutions, exhibiting an overall higher quality solution. In order to demonstrate this, the percentages of positioning errors that are larger than 50 metres for each algorithm are given in Table 2.

	<i>East (%)</i>	<i>North (%)</i>	<i>Height (%)</i>
Least-squares	8.6	9.6	33.8
“Top down”	7.8	22.5	36.0
“Bottom up”	2.2	8.8	25.6

Table 2: Percentage of positioning errors greater than 50m, produced by the three algorithms during test 1

As can be seen from the table, the “Bottom up” consistency algorithm achieves, respectively, 74%, 8% and 24% reductions in the number of easting, northing and height errors exceeding 50m compared to conventional least-squares. The “Top down” algorithm in this respect, however, performs worse than the conventional solution, indicating that it frequently converges on the wrong self-consistent subset of measurements.

Nevertheless, occasional erroneous solutions are still obtained from the “Bottom up” consistency-checking algorithm. This is because, at those particular epochs, only a few or even zero inliers could be found with the best MSS set. The final solutions were exact solutions produced using only the minimum number of 5 mixed GPS and GLONASS satellites. This indicates that either the assumed best MSS was actually biased, i.e. that the cost function needs further improvement, or that there were not enough “clean” signals to produce good solutions.

This can be further clarified by introducing a 10-metre accuracy height aiding measurement obtained from a 3D city model. For this test, the height aiding error is at a known level, and the height is effectively one additional ranging measurement from the centre of the Earth, which helps by improving the geometry of the set of ranging measurements. One additional range measurement and an improved geometry would help to improve the performance if the erroneous solutions are due to their being insufficient “clean” signals, whereas less improvement is expected if the errors are due to a suboptimal cost function. The effects of introducing height aiding are shown in Table 3 and Table 4.

	<i>dE (m)</i>	<i>dN (m)</i>	<i>dH (m)</i>
Least-squares	23.0	15.1	5.3
“Bottom up”	19.3	14.3	5.4

Table 3: The RMS positioning error with height aiding for test 1

	<i>East (%)</i>	<i>North (%)</i>	<i>Height (%)</i>
Least-squares	7.9	2.1	0.0
“Bottom up”	1.8	1.0	0.0

Table 4: Percentage of positioning errors greater than 50m, produced with height aiding during test1

As can be seen from the tables, while limited improvements can be seen from the easting RMS errors, the RMS error in northing is improved dramatically. In Table 1 and 3, it is also very clear that further improvement is achieved reducing the number of erroneous solutions from Table 2 and 4. The percentage of erroneous solution in the north direction is further reduced by 88%. This shows that for this particular test, the number of “clean” signals available was the main limiting factor affecting the performance of the “Bottom up” consistency-checking algorithm.

4.2. TEST 2

The second test data set was collected near Fenchurch Street on 23rd July 2012. The duration of the data is 10 minutes. Figure 6 shows a comparison of the position solutions produced with the three algorithms. The yellow pin in the picture marks out the truth point, G004. This was established using a 3D city model with tape measurements from landmarks, which is accurate at decimetre-level. The solution markings follow the same convention as Figure 4. The smaller circle has a 10-metre radius, and the larger circle a 20-metre radius.

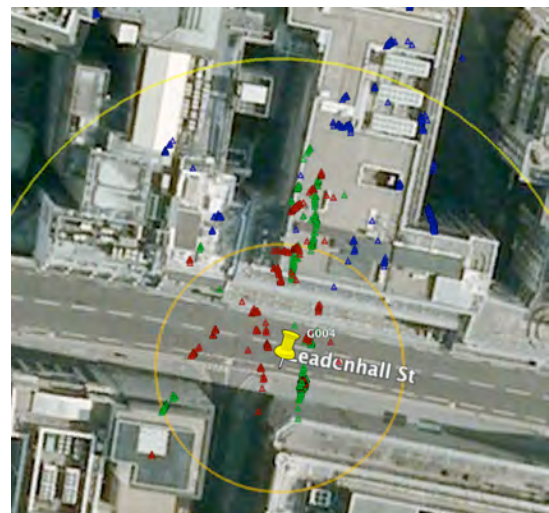


Figure 6: The positioning solution for test 2

The overall positioning error of all three algorithms is shown in Figure 7. The colouring convention follows Figure 5. The RMS positioning errors are also expressed

as easting, northing and height in Table 5. The percentages of erroneous positioning errors for each algorithm are given in Table 6, noting that the erroneous positioning error is defined as larger than 20 metres for this test.

From the RMS and percentages of erroneous errors information shown in Tables 5 and 6, neither of the two consistency checking algorithms significantly outperforms the conventional method. The “Top down” algorithm performs significantly worse than the other two methods. The “Bottom down” algorithm in general achieves a similar level of performance to the conventional method with occasional improvement in the height direction.

However, another side of the story can be told from a close examination of Figure 7. As shown in the figure, the performance of the “Bottom up” algorithm is significantly better than other two algorithms in the first 5 minutes. The level of performance for the last 5 minutes however, is degraded to a similar or even slightly worse level than the conventional method.

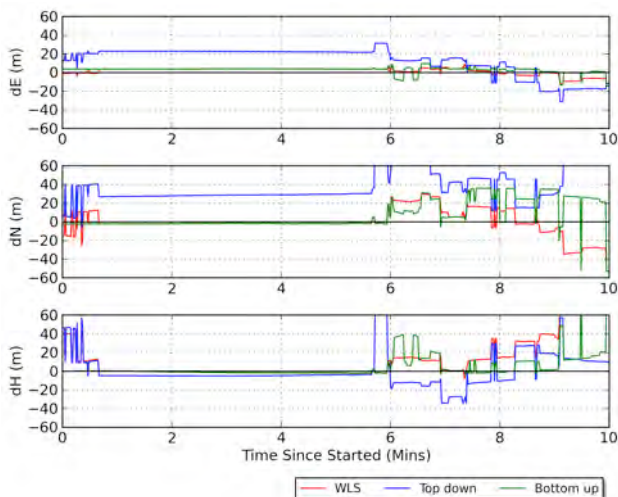


Figure 7: The positioning error comparison of three algorithm for test 2

	$dE (m)$	$dN (m)$	$dH (m)$
Least-squares	4.2	13.6	31.3
“Top down”	19.58	45.98	18.17
“Bottom up”	4.3	16.3	12.9

Table 5: The RMS positioning error comparison of the three algorithms for test 2

	<i>East (%)</i>	<i>North (%)</i>	<i>Height (%)</i>
Least-squares	0.0	17.7	20.3
“Top down”	61.0	92.6	15.1
“Bottom up”	0.0	27.7	6.7

Table 6: Percentage of positioning errors greater than 20m, produced by the three algorithms during test 2

First of all, the constellation status was different for the two halves of data. The fact that the conventional least-

squares solution performed better at times during the second half of the data set indicates that it is likely that the “Bottom up” consistency-checking method was converging on the wrong subsets of signals as the “Top down” method is prone to do. This hypothesis is supported by again introducing a 10-metre-accuracy height aiding measurement.

	$dE (m)$	$dN (m)$	$dH (m)$
Least-squares	6.3	16.7	6.3
“Bottom up”	4.8	15.8	5.7

Table 7: The RMS positioning error with height aiding for test 2

	<i>East (%)</i>	<i>North (%)</i>	<i>Height (%)</i>
Least-squares	1.2	18.6	0.0
“Bottom up”	0.7	30.6	0.0

Table 8: Percentage of positioning errors greater than 20m, produced with height aiding during test2

Table 7 and 8 show the effect of introducing height aiding on the second test data. No visible improvement from introducing height aiding can be observed. This supports the hypothesis that the algorithm was converging on the wrong subset of data due to a suboptimal cost function.

5. CONCLUSIONS AND FUTURE WORK

A new RANSAC-based “Bottom up” approach for using consistency checking to mitigate GNSS NLOS and multipath errors has been explored in this paper. The positioning performance of the new algorithm and conventional methods has been compared in difficult urban environments. In addition, the effect of using height aiding at the final MSS and CS solution level has been investigated.

The test results demonstrate accuracy improvement of the new method over conventional methods and, more importantly, an improved resilience to erroneous urban GNSS positioning errors. Occasional performance degradation, however, can still be observed when there is either a limited number of “clean” signals available or the algorithm converges on the wrong subset of signals. The introduction of height aiding demonstrates significant further performance enhancement for the first situation, but has little effect on the second.

For future improvement of the new algorithm, it is clear that in order to deal with incidences of wrong convergence, it is necessary to further improve the existing cost function. Extra information, such as elevation and street orientation, or even NLOS error characteristics could be brought into the formulation of a new cost function.

Furthermore, while the height aiding information is currently only used to aid the final solution, it may be worth incorporating the additional measurement into the MSS evaluation stage as well as producing the final

solution. So that the improved MSS “residuals” can provide more information on the consistency among measurements.

The current algorithm exhibits the ability to improve along street solutions. By combining the new algorithm with other techniques such as shadow matching [12], an approach known as intelligent urban positioning, it is possible to achieve an overall improvement in performance [11].

ACKNOWLEDGEMENTS

This work is part of the Innovative Navigation using new GNSS Signals with Hybridised Technologies (INSIGHT) program. INSIGHT (www.insight-gnss.org) is a collaborative research project funded by the UK’s Engineering and Physical Sciences Research Council (EPSRC) to extend the applications and improve the efficiency of positioning through the exploitation of new global navigation satellite systems signals. It is being undertaken by a consortium of twelve UK university and industrial groups: Imperial College London, University College London, the University of Nottingham, the University of Westminster, EADS Astrium, Nottingham Scientific Ltd, Leica Geosystems, Ordnance Survey of Great Britain, QinetiQ, STMicroelectronics, Thales Research and Technology UK Limited, and the UK Civil Aviation Authority.

The authors would like to thank the following people who assisted the data collection for test 1: Mr Chris Atkins, Mr Toby Webb and Ms Chian-yuan Naomi Li. Especial gratitude is also expressed to Mr Lei Wang, who helped to provide the truth information for test 2 and design the data collection.

REFEREMCES

- [1] Wang, L., P. D. Groves, and M. K. Ziebart, “Multi-Constellation GNSS Performance Evaluation for Urban Canyons Using Large Virtual Reality City Models,” *Journal of Navigation*, Vol. 65, No. 3, 2012.
- [2] Groves, P.D., *Principles of GNSS, Inertial, and Multisensor Integrated Navigation Systems*, Artech House, 2008.
- [3] Braasch, M. S., “Multipath Effects,” In *Global Positioning System: Theory and Applications Volume I*, pp. 547–568, Parkinson, B. W. and Spilker, J. J., Jr (eds), Washington, DC: AIAA, 1996.
- [4] Van Nee, R. D. J., “GPS Multipath and Satellite Interference,” *Proc. ION 48th AM*, Washington, DC, June 1992, pp. 167–177.
- [5] Brown, A., and Gerein, N., “Test Results from a Digital P(Y) Code Beamsteering Receiver for Multipath Minimization,” *Proc. ION 57th AM*, Albuquerque, NM, June 2001, p. 872–878.
- [6] Lau, L. and P. Cross, “Investigations into Phase Multipath Mitigation Techniques for High Precision Positioning in Difficult Environments”, *Journal of Navigation*, Vol. 60, No.3, 2007, pp. 457-482.
- [7] Groves, P. D., Z. Jiang, B. Skelton, P. A. Cross, L. Lau, Y. Adane and I. Kale, “Novel Multipath Mitigation Methods using a Dual-polarization Antenna,” *Proc. ION GNSS 2010*, Portland, OR.
- [8] Keshvadi, M. H., A. Broumandan, and G. Lachapelle, “Analysis of GNSS Beamforming and Angle of Arrival Estimation in Multipath Environments,” *Proc ION ITM*, San Diego, CA, January 2011, pp. 427-435.
- [9] Marais, J., M. Berbineau, and M. Heddebaut, “Land Mobile GNSS Availability and Multipath Evaluation Tool,” *IEEE Transactions on Vehicular Technology*, Vol. 54, No. 5, 2005, pp. 1697–1704.
- [10] Meguro, J., et al., “GPS Multipath Mitigation for Urban Area Using Omnidirectional Infrared Camera,” *IEEE Transactions on Intelligent Transportation Systems*, Vol. 10, No. 1, 2009, pp. 22–30.
- [11] Groves, P. D., Z. Jiang, L. Wang, and M. K. Ziebart, “Intelligent Urban Positioning using Multi-Constellation GNSS with 3D Mapping and NLOS Signal Detection,” *Proc. ION GNSS 2012*.
- [12] Wang, L., P. D. Groves, and M. K. Ziebart, “GNSS Shadow Matching: Improving Urban Positioning Accuracy Using a 3D City Model with Optimized Visibility Prediction Scoring,” *Proc. ION GNSS 2012*.
- [13] Feng, S., Ochieng, W.Y., Walsh, D and Ioannides, R., “A Measurement Domain Receiver Autonomous Integrity Monitoring Algorithm”. *GPS Solutions*, Springer, 10(2), (2006), 85-96.
- [14] Feng, S., Ochieng, W.Y., “User Level Autonomous Integrity Monitoring for Seamless Positioning in All Conditions and Environments”, *Proceedings of the European Navigation Conference*, Manchester, 7-10, May, 2006.
- [15] Jiang, Z., P. D. Groves, W. Y. Ochieng, S. Feng, C. D. Milner, and P. G. Mattos, “Multi-Constellation GNSS Multipath Mitigation Using Consistency Checking,” *Proc. ION GNSS 2011*, Portland, OR, pp.3889–3902.
- [16] Torr, P.H.S., Zisserman, A., “MLESAC: A New Robust Estimator with Application to Estimating Image Geometry”, *Computer Vision and Image Understanding*, Vol. 78, No. 1, 2000, pp.138-156